



**University of
Zurich**^{UZH}

**Zurich Open Repository and
Archive**

University of Zurich
Main Library
Strickhofstrasse 39
CH-8057 Zurich
www.zora.uzh.ch

Year: 2016

Radiocarbon in dissolved organic carbon of the Atlantic Ocean

Druffel, Ellen R M ; Griffin, Sheila ; Coppola, Alysha I ; Walker, Brett D

Abstract: Marine dissolved organic carbon (DOC) is produced in the surface ocean though its radiocarbon (^{14}C) age in the deep ocean is thousands of years old. Here we show that >10% of the DOC in the deep North Atlantic is of post-bomb origin and that the ^{14}C age of pre-bomb DOC is >4900 ^{14}C yr, 900 ^{14}C yr older than previous estimates. We report ^{14}C ages of DOC in the deep South Atlantic that are intermediate between values in the North Atlantic and the Southern Ocean. Finally, we conclude that DOC ^{14}C ages are older and a portion of deep DOC is more dynamic than previously reported.

DOI: <https://doi.org/10.1002/2016GL068746>

Posted at the Zurich Open Repository and Archive, University of Zurich

ZORA URL: <https://doi.org/10.5167/uzh-124082>

Journal Article

Accepted Version

Originally published at:

Druffel, Ellen R M; Griffin, Sheila; Coppola, Alysha I; Walker, Brett D (2016). Radiocarbon in dissolved organic carbon of the Atlantic Ocean. *Geophysical Research Letters*, 43(10):5279-5286.

DOI: <https://doi.org/10.1002/2016GL068746>

1 Radiocarbon in dissolved organic carbon of the Atlantic Ocean

2

3 by

4 E. R. M. Druffel, S. Griffin, A. I. Coppola, and B. D. Walker

5 Department of Earth System Science, U. C. Irvine, Irvine, CA 92697–3100

6 Resubmitted to *Geophysical Research Letters* March 2016

7

8 **Abstract** Marine dissolved organic carbon (DOC) is produced in the surface ocean though its
9 radiocarbon (^{14}C) age in the deep ocean is thousands of yr old. Here we show that $\geq 10\%$ of the
10 DOC in the deep North Atlantic is of post-bomb origin and that the ^{14}C age of pre-bomb DOC is
11 ≥ 4900 ^{14}C yr, ~ 900 ^{14}C yr older than previous estimates [*Druffel et al.*, 1992]. We report ^{14}C
12 ages of DOC in the deep South Atlantic that are intermediate between values in the North
13 Atlantic and the Southern Ocean. Finally, we conclude that DOC ^{14}C ages are older and a portion
14 of deep DOC is more dynamic than previously reported.

15

16

17 **1. Introduction**

18 Marine DOC is the largest pool of reduced carbon (C) in the oceans, about equal to the
19 atmospheric CO₂ reservoir. Though most DOC is produced from photosynthetic uptake of
20 modern DIC in the surface ocean, the bulk ¹⁴C ages in deep open ocean DOC ranged from 4000
21 ¹⁴C yr in the Sargasso Sea to 6000 ¹⁴C yr in the North and South Pacific [*Druffel and Griffin,*
22 2015; *Druffel et al.*, 1992; *Williams and Druffel*, 1987]. The deep Southern Ocean DOC ¹⁴C age
23 (5600 ¹⁴C yr) was much closer to that in the deep Pacific, suggesting that the North Atlantic
24 DOC contained bomb ¹⁴C, there was a source of old DOC to the Southern Ocean [*Druffel and*
25 *Bauer*, 2000] or diverse sources of DOC [*Follett et al.*, 2014]. In the ocean margins, there is
26 evidence of inputs of old DOC in the deep northeast Pacific and the mid-Atlantic Bight off the
27 US coast [*Bauer and Druffel*, 1998] and young DOC to the deep subpolar North Pacific [*Tanaka*
28 *et al.*, 2010]. Terrestrially-derived DOC was found in the deep Arctic Ocean [*Griffith et al.*,
29 2012].

30

31 We find that the DOC $\Delta^{14}\text{C}$ in the deep Sargasso Sea in 2012 was lower than it was in 1989,
32 indicating that bomb ¹⁴C levels had decreased over a period of two decades. Implications for the
33 C cycle in the ocean include the presence of a labile pool of DOC in deep water.

34

35 **2. Methods**

36 Water samples were collected from the North and South Atlantic Ocean during the Repeat
37 Hydrography CLIVAR (Climate Variability and Predictability) program. Sampling included
38 surface and subsurface water, northward Antarctic Intermediate Water (AAIW ~700–1200 m,
39 low salinity, high silica) and Upper Circumpolar Deep Water (1000-2000 m), southward North

40 Atlantic Deep Water (NADW 1500–4000 m, high oxygen, low silica), and Antarctic Bottom
41 Water (within a few hundred meters of the bottom, cold and dense) [*Jenkins et al.*, 2015a; *Reid*,
42 1989]. A data-constrained ocean circulation model was used to show that in the South Atlantic,
43 Antarctic water penetrates the NADW in volume-weighted averages that vary from 20-40%
44 [*DeVries and Primeau*, 2011].

45
46 Radiocarbon in DOC was measured in seawater samples collected from 3 stations along 32°S on
47 the A10 cruise in October 2011, 4 stations along 20°W on the A16N cruise in July/August 2013,
48 and 4 stations along 65°W on the A22 cruise in March/April 2012 (Figure 1 insets, Table S1 in
49 the supporting information). Samples shallower than 400 m were filtered using precombusted
50 GFF (0.7 μ M) filters, and all samples were collected in 1L Amber Boston Round glass bottles,
51 and frozen at –20°C at an angle to avoid breakage until analysis at U.C. Irvine (UCI). Samples
52 were diluted with 18.2 M Ω Milli-Q water (DOC concentration 0.5–0.9 μ M), acidified to pH 2
53 with 85% phosphoric acid, purged with ultra high purity helium gas (UHP 5.0) and UV-oxidized
54 (UVox) [*Beaupré et al.*, 2007; *Druffel et al.*, 2013; *Griffin et al.*, 2010]. Samples for DIC $\Delta^{14}\text{C}$
55 analyses were prepared according to standard methods [*McNichol et al.*, 1994].

56
57 The resultant CO₂ from UVox was converted to graphite on iron catalyst for ¹⁴C analysis at the
58 Keck Carbon Cycle Accelerator Mass Spectrometry (AMS) Laboratory at UCI [*Southon et al.*,
59 2004; *Xu et al.*, 2007]. Total uncertainties for individual DOC $\Delta^{14}\text{C}$ values of approximately
60 –500‰ are $\pm 4\%$ as determined from analyses of numerous duplicate seawater samples and
61 secondary standards [*Druffel et al.*, 2013]. Total uncertainty for DIC $\Delta^{14}\text{C}$ values are $\pm 3\%$.
62 Total uncertainties for DOC concentrations are $\pm 1.0\mu\text{M}$. Stable C isotopes were measured on

63 splits of the CO₂ samples using a Thermo Electron Delta Plus mass spectrometer; total
64 uncertainty of δ¹³C values are ±0.2‰.

65

66 **3. Results**

67 **3.1 DOC Δ¹⁴C and δ¹³C Values**

68 In the North Atlantic, the surface DOC Δ¹⁴C values ranged from −306‰ at 60°N to −223‰ at
69 20°N (Fig. 1a,b and Table S2 in the supporting information). Surface values ranged from −279‰
70 to −259‰ in the South Atlantic (Fig. 1c). Minimum Δ¹⁴C values were reached by ~800–1100m
71 depth (AAIW) in the North (−441‰ to −395‰) (Figure 1a,b) and South (−477‰ to −466‰,
72 Figure 1c) Atlantic. Generally, the DOC Δ¹⁴C values below 1200m in the North Atlantic
73 decreased with depth. Two values from 2569 and 3576m depth in the northeast Atlantic (32°N)
74 were the lowest (−460‰ and −462‰, respectively) and a value (−370‰) from 1313m depth at
75 the farthest north site (60°N) was the highest (Fig. 1b). The average of deep (>1800m) DOC
76 Δ¹⁴C values from the same location (within 145 km) in the Sargasso Sea are 19‰ higher in 1989
77 (−396±10‰ n=6) than those in 2012 (−415±8‰ n=5) (Fig. 1a).

78

79 The DOC Δ¹⁴C values from the South Atlantic below 1200m averaged −471±2‰ (n=19), and
80 were significantly lower than those in the North Atlantic. Values below 3500 m depth were
81 significantly higher in the southeast basin (−464 ± 4‰ n=3) than those in the southwest basin
82 (−482 ± 3‰ n=3) (Fig. 1c).

83

84 Stable C isotope (δ¹³C) DOC values ranged between −20.5 and −23.0‰, typical of marine
85 produced organic matter (Figure S1 in the supporting information). Values were higher in the

86 deep South Atlantic ($-21.3 \pm 0.2\text{‰}$ $n=13$) and Sargasso Sea ($-20.8 \pm 0.3\text{‰}$ $n=4$) than those in
87 the rest of the deep North Atlantic ($-22.3 \pm 0.1\text{‰}$ $n=19$).

88

89 **3.2 DOC Concentrations**

90 Concentrations of DOC ranged from 58–76 μM in the upper 40m of the water column (Fig. S2
91 and Table S2 in the supporting information). Values decreased to about 1000m depth at all
92 stations, and average values in the deep Atlantic were significantly lower in the south (38.1 ± 1.1
93 μM $n=22$) than in the north ($40.9 \pm 1.3 \mu\text{M}$ $n=23$) (Figure S2 in the supporting information).

94

95 **3.3 DIC $\Delta^{14}\text{C}$ Values**

96 New DIC $\Delta^{14}\text{C}$ values are available for the South Atlantic samples (2011) and 2 depths from the
97 Sargasso Sea station (2012) (Figure 1d). Surface DIC $\Delta^{14}\text{C}$ values ranged from +47–54‰ in the
98 South Atlantic and was +58‰ in the Sargasso Sea. Values in the South Atlantic decreased
99 steadily to ~1000m depth and averaged -127‰ below 1200m. Values in the southwest basin
100 were higher at 2400m and 3100m, and lower at 3900 and 4300m, than those in the southeast
101 basin, which did not vary with depth below 2000m.

102

103 **4. Discussion**

104 We address three major trends in the DOC $\Delta^{14}\text{C}$ data. First, values in the deep North Atlantic
105 varied both temporally and spatially, indicating of the presence of bomb ^{14}C . Second, the
106 decrease of pre-bomb DOC $\Delta^{14}\text{C}$ values between the deep North and deep South Atlantic are
107 discussed as possible aging of DOC during the southward transport of NADW. Third, we
108 discuss the possible reasons for the dissimilarity of the deep DOC $\Delta^{14}\text{C}$ values in the southwest

109 and southeast basins of the Atlantic. Fourth, the global trends of DOC $\Delta^{14}\text{C}$ values in the open
110 ocean are presented and discussed.

111

112 **4.1 Bomb ^{14}C in North Atlantic DOC and Decadal Variability**

113 There was a wide range of DOC $\Delta^{14}\text{C}$ values (-462‰ to -370‰) in the deep North Atlantic
114 below 1200m (Figure 1a,b). Values were highest in the northernmost station (60°N) and lowest
115 in the northeast station at 32°N . This pattern is not surprising because NADW forms by surface-
116 to-deep convection in the Labrador and the Nordic Seas, incorporating bomb ^{14}C into DIC of the
117 Deep Western Boundary Current [*Key et al.*, 2004; *Stuiver and Ostlund*, 1980]. It stands to
118 reason that bomb ^{14}C would also be present in DOC in the Sargasso Sea during the 1989 cruise.
119 Notwithstanding, there were six very low DOC $\Delta^{14}\text{C}$ values, the three deepest samples from
120 32°N (-460 , -462‰ , -452‰) and the deepest sample from 45°N (-453‰) in the northeast
121 Atlantic, and the two deepest samples from 20°N in the Puerto Rican Trench (-452‰ , -456‰)
122 in the northwest Atlantic (Figure 1a,b and Table S2 in the supporting information). The DOC
123 concentrations of these 6 samples (average $38.9\pm 2.1\mu\text{M}$) are not significantly different from the
124 remaining deep samples at these sites (average $40.5\pm 1.9\mu\text{M}$ $n=9$). We hypothesize that the
125 average of the six low $\Delta^{14}\text{C}$ values ($-456\pm 4\text{‰}$) represents an upper bound estimate of the pre-
126 bomb DOC $\Delta^{14}\text{C}$ in the North Atlantic. This is supported by minimal bomb-produced tritium
127 ($\delta^3\text{H} < 0.08$ TU) at these deep locations [*Jenkins*, 2007; *Jenkins et al.*, 2015b]. This value is 66%
128 lower than the previous estimate for the deep North Atlantic DOC $\Delta^{14}\text{C}$ value from samples
129 collected in 1989 (-396‰) [*Druffel et al.*, 1992].

130

131 We estimate the fraction of post-bomb DOC in the deep north Atlantic in 2012–2013 using a
132 mass balance calculation. Assuming the source of bomb ^{14}C to the deep water was from
133 solubilization of organic particles produced in the surface (DIC in the surface waters during the
134 period 1992-2012 averaged 70‰ (Druffel, unpublished data)), and the deep average DOC $\Delta^{14}\text{C}$
135 value was -415‰ ($>1800\text{m}$, excluding pre-bomb values), there was 89% pre-bomb DOC
136 (-456‰) and 11% post-bomb DOC from organic particles ($-415\text{‰} = 0.89 \cdot -456\text{‰} + 0.11 \cdot$
137 70‰). Thus, the input of post-bomb DOC to the deep north Atlantic was $> 11\%$ of the standing
138 stock of the deep DOC. A similar calculation for the Sargasso Sea site in 1989, assuming the
139 DIC $\Delta^{14}\text{C}$ in the surface waters during the previous two decades was $+140\text{‰}$ [Druffel, 1989],
140 reveals that there was $\leq 90\%$ pre-bomb DOC and $\geq 10\%$ post-bomb DOC from organic particles
141 ($-396\text{‰} = 0.90 \cdot -456\text{‰} + 0.10 \cdot 140\text{‰}$).

142

143 We observed a temporal shift in DOC $\Delta^{14}\text{C}$ values in the deep Sargasso Sea. Here, the average
144 deep value was 19‰ higher in 1989 than in 2012. This decrease was likely not the result of a
145 change in the production of NADW, which has not changed in the last decade [Fischer *et al.*,
146 2010]. Also, seasonal variability of the deep sea DOC pool is unlikely, because deep ocean
147 DOC $\Delta^{14}\text{C}$ time series have not observed temporal changes [Bauer *et al.*, 1998; Beaupré and
148 Druffel, 2009]. Input of aged DOC from hydrothermal systems is also not likely the cause of the
149 decrease in deep DOC $\Delta^{14}\text{C}$ in the Atlantic given low $\delta^3\text{H}$ values in these waters (Figure S3 in
150 the supporting information). We hypothesize that the 19‰ higher average DOC $\Delta^{14}\text{C}$ value in
151 1989 represents a higher relative contribution of bomb ^{14}C to the DOC pool than was present in
152 2012–2013.

153

154 To test this hypothesis, we compare the amount of post-bomb DOC in the deep Sargasso Sea in
155 1989 to net production of organic C exiting the surface ocean. If we assume that a minimum of
156 10% of the C exported from the mixed layer at the BATS site (32°10'N 64°30'W) was converted
157 to DOC ($0.10 \cdot 3 \pm 1 \text{ mole C m}^{-2} \text{ yr}^{-1} = 0.30 \text{ mole C m}^{-2} \text{ yr}^{-1}$) [Emerson, 2014], then the
158 replacement time of the DOC in a 1 m² area of the deep ocean ($2500 \text{ m}^3 \cdot 0.043 \text{ mol m}^{-3} = 108$
159 mol C) (see Table S2 in the supporting information) would have been 360 yr ($108 \text{ mol C m}^{-2} /$
160 $0.30 \text{ mole C m}^{-2} \text{ yr}^{-1}$). To replace 10% of the DOC in a 1 m² area of the deep ocean would have
161 taken about 36 yr ($0.10 \cdot 360 \text{ yr}$), which is approximately equal to the time that bomb ¹⁴C had
162 been in the ocean from the time of the first sampling of DOC in the Sargasso Sea (1989–1957 =
163 32 yr). This simple calculation indicates that DOC in the deep Sargasso Sea is likely a
164 heterogeneous mixture that contains distinct $\Delta^{14}\text{C}$ signatures with different cycling rates. We
165 determine that $\geq 4\mu\text{M}$ DOC has ages of 10–30 yr (post-bomb) and $\leq 39\mu\text{M}$ has ages of centuries.
166 This has important implications for the role of DOC in the oceanic C cycle of the Atlantic (see
167 Section 5).

168
169 Evidence that deep DOC is a heterogeneous, isotopic mixture in the surface ocean is shown by a
170 Keeling plot (Figure S4 in the supporting information), which identifies the $\Delta^{14}\text{C}$ value of an
171 excess component added to a background pool [Mortazavi and Chanton, 2004]. Keeling plots of
172 DOC concentration⁻¹ versus DOC $\Delta^{14}\text{C}$ value were linear, and suggested rapid export out of the
173 upper 85m, and advection between 100–1000m [Beaupré and Aluwihare, 2010]. Keeling plots of
174 the Atlantic data reveal y-intercepts that were similar to the DIC $\Delta^{14}\text{C}$ of the surface waters at
175 each site (Table S3 in the supporting information), indicating that the excess DOC originated
176 from recent production in the surface ocean. Similar results were obtained from Keeling plots of

177 South Pacific data [*Druffel and Griffin, 2015*] (Figure S4 and Table S3 in the supporting
178 information).

179

180 Additionally, DOC $\delta^{13}\text{C}$ values in the North Atlantic (1989–2013) were generally lower than
181 those in the South Atlantic (Figure S1 of the supporting information), which may indicate that
182 there is a larger ^{13}C Suess Effect (presence of mostly fossil fuel-derived CO_2) in the deep North
183 Atlantic than that in the South Atlantic. This would support the premise that bomb ^{14}C was
184 present in the North Atlantic, however it is also possible that input of fossil carbon may have
185 contributed to a decrease in DOC $\Delta^{14}\text{C}$ values in the North Atlantic.

186

187 **4.2 Aging of DOC in North Atlantic Deep Water**

188 Our estimate of the upper bound for the pre-bomb DOC $\Delta^{14}\text{C}$ value in the deep North Atlantic (–
189 $456\pm 4\%$ section 3.3.1) corresponds to a ^{14}C age of 4900 ± 60 ^{14}C yr. This means that the pre-
190 bomb ^{14}C ages of the deep basins of the North Atlantic and North Pacific have decreased from
191 4000 ^{14}C and 6000 ^{14}C yr, to 4900 and 6000 ^{14}C yr.

192

193 The difference between the pre-bomb ^{14}C ages of the North (4900 ± 60 ^{14}C yr) and South
194 (5120 ± 35 ^{14}C yr) Atlantic DOC is 220 ± 95 ^{14}C yr. This difference is equal to the estimated
195 replacement time (250 ^{14}C yr) determined from the deep DIC ^{14}C ages in the Atlantic [*Stuiver et*
196 *al.*, 1983]. However, this may be fortuitous due to the presence of bomb (and possibly pre-bomb)
197 DOC from the dissolution of surface particles [*Smith et al.*, 1992a] in the deep waters. This
198 similarity may indicate that DOC has been transported with NADW as it traveled southward, but
199 we cannot demonstrate this because DOC is not an isolated pool.

200
201
202
203
204
205
206
207
208
209
210
211
212
213
214
215
216
217
218
219
220
221
222

4.3 Spatial Variability of $\Delta^{14}\text{C}$ in the Deep South Atlantic

Comparison of the DOC and DIC $\Delta^{14}\text{C}$ values from the South Atlantic in 2011 reveals that both were high in the upper 1000 m indicating presence of bomb ^{14}C (Figure 1c,d). Bomb ^{14}C penetration was several hundred meters deeper in the DIC pool. In the two deepest samples (3900 and 4300 m), the DIC $\Delta^{14}\text{C}$ values in the southwest basin were 9‰ and 22‰ lower than those in the southeast basin (Fig. 1d). Older waters in the west suggest that they may be less well-ventilated than those in the east. The DOC $\Delta^{14}\text{C}$ values from the west were also lower (by 11-24‰) in the deepest three samples (3500–4300m) than those in the east (Fig. 1c).

Higher $\Delta^{14}\text{C}$ values of DIC and DOC in the deep southeast basin could be the result of dissolution of high $\Delta^{14}\text{C}$ particulate organic carbon (POC) from the surface, or mixing of Southern Ocean waters into the deep South Atlantic. The amount of surface POC (pre-bomb $\Delta^{14}\text{C}$ value of -70‰ [Druffel, 1996]) required to increase the deep DOC $\Delta^{14}\text{C}$ value from -483‰ (west basin average) to -463‰ (east basin average) is 5% of the DOC pool. This value would be 4% if the surface POC $\Delta^{14}\text{C}$ value contained bomb ^{14}C ($+70\text{‰}$). We note that net primary production is higher in the southeast Atlantic than that in the southwest Atlantic [Falkowski, 2014], which would cause a higher input of surface-derived POC to the deep southeast basin, and provide a mechanism for the higher DOC $\Delta^{14}\text{C}$ values. Second, DeVries and Primeau (2011) used a data-constrained ocean circulation model to characterize the distribution of water masses and their ages in the global ocean and showed that the ratio of Southern Ocean to NADW at 32°S

223 in the South Atlantic was about 1:3. There was no evidence that this ratio was different in the
224 southeast and southwest basins (F. Primeau, personal communication). Thus, we are not able to
225 determine if dissolution of POC to DOC or physical mixing is the reason for the DIC and DOC
226 $\Delta^{14}\text{C}$ offsets we observe between the southwest and southeast basins of the Atlantic.

227

228 **4.4 Global Trends of DOC $\Delta^{14}\text{C}$ Values**

229 There are seventeen DOC $\Delta^{14}\text{C}$ profiles available for the Pacific and Atlantic Ocean basins,
230 including the nine new profiles presented here. Though the number of profiles is limited, they
231 improve our understanding of the global ocean DOC $\Delta^{14}\text{C}$ cycle. To portray the global DOC $\Delta^{14}\text{C}$
232 trends better, a 3-dimensional animation is presented that displays the $\Delta^{14}\text{C}$ profiles in these
233 basins [*Schlitzer, 2015*] ([DOC 14C animation](#)). The animation shows the gradual decrease of
234 DOC $\Delta^{14}\text{C}$ values in the deep water, from high values in the far North Atlantic (-410‰ green) to
235 lower values in the South Atlantic (-470‰ aqua). There are areas of low $\Delta^{14}\text{C}$ values (-456‰
236 turquoise) in the northwest at 20°N and the northeast Atlantic, portraying the water masses we
237 hypothesize as pre-bomb DOC in these slower ventilated regions.

238

239 The $\Delta^{14}\text{C}$ values decreased further at the Southern Ocean site (-500‰ blue), and fell to an even
240 lower value (-525‰ purple) in the South and North Pacific basins. As noted above, the
241 surprising lack of a gradient in $\Delta^{14}\text{C}$ values in the Pacific basin indicates that processes other
242 than ^{14}C decay during northward transport are at work [*Druffel and Griffin, 2015*]. Values were
243 lowest (-550‰ fuchsia) off California in the northeast Pacific, and were believed to have been
244 influenced by sources of old C from the continental margin [*Bauer and Druffel, 1998*]. The
245 surface waters at all locations were similar (average $-255\pm 35\text{‰}$ $n=18$), with the exception of the

246 Southern Ocean ($-372 \pm 5\%$ n=3) where surface-to-deep mixing bring lower $\Delta^{14}\text{C}$ water to the
247 surface.

248

249 The gradual decrease of deep DOC $\Delta^{14}\text{C}$ values from the North Atlantic to the South Atlantic
250 suggests that most of the DOC ages as it is transported southward in NADW. This aging is
251 portrayed in Figure 3, which shows DOC concentrations versus ^{14}C ages for each site in the
252 Atlantic, SOce and the Pacific ($>1500\text{m}$). The decrease in DOC concentration and ^{14}C ages from
253 the North Atlantic to the Pacific mimics the flow of NADW along the deep ocean conveyor, and
254 is lowest for both quantities in the Pacific basin. This general decrease agrees with previous
255 studies of global deep DOC concentrations along the deep ocean conveyor [*Hansell et al.*, 2012].
256 The SOce values lie off of this relationship suggesting an additional source of DOC [*Druffel and*
257 *Bauer*, 2000] or different isotopic signatures within deep DOC [*Follett et al.*, 2014].

258

259 An estimate of the transport time of most of the DOC from the northern North Atlantic to the
260 Southern Ocean, assuming decay of ^{14}C in DOC is the major cause of the gradient, is
261 approximately 670 ^{14}C yr (5570 minus 4900 ^{14}C yr). The transport time of DOC from the
262 Southern Ocean to the Pacific basin is approximately 400 ^{14}C yr (5970 minus 5570 ^{14}C yr).
263 Thus, the total time of transport of deep DOC from the northern North Atlantic to the Pacific
264 basin is approximately 1080 ^{14}C yr. This value is similar to the sum of the deep water
265 replacement times for DIC in the Atlantic and the Pacific (250 + 510 = 760 yr) [*Stuiver et al.*,
266 1983]. These estimates do not account for the change of DIC and DOC in the deep water by
267 particle dissolution and remineralization, which would make the transport time estimates too
268 low. They also ignore preferential remineralization of DOC that has different $\Delta^{14}\text{C}$ values from

269 the bulk value. As one would expect younger (higher $\Delta^{14}\text{C}$), more labile DOC to be
270 remineralized preferentially, this would cause the transport time estimates determined above to
271 be too high.

272

273 **5. Implications for the DOC Cycle in the Ocean**

274 Though the bulk DOC ages in the deep sea are thousands of ^{14}C yr old, we show that a portion of
275 this DOC is post-bomb, and that the $\Delta^{14}\text{C}$ values in the deep Sargasso Sea have changed on
276 decadal time scales. We estimate that the pre-bomb age of DOC in the North Atlantic (4900 ^{14}C
277 yr) is older than previously reported (4000 ^{14}C yr [Druffel *et al.*, 1992]). These results change our
278 current understanding of labile vs. refractory DOC in the deep ocean.

279

280 Whereas $\geq 10\%$ of the DOC in the deep North Atlantic is of post-bomb origin, $\leq 90\%$ of the DOC
281 has an older ^{14}C age of 4900 ^{14}C yr. There is a fraction of the pre-bomb DOC that has ^{14}C ages
282 much greater than the timescale of meridional overturning circulation. Ancient DOC has been
283 identified in ultrafiltered DOC as black C with ages of 18000 to 21800 ^{14}C yr [Ziolkowski and
284 Druffel, 2010]. Whether this ancient DOC was put into the ocean pre-aged (e.g. hydrothermal
285 sources), or had aged by decay within the deep sea, is an open question.

286

287 Though the ^{14}C age of pre-bomb DOC in the North Atlantic was ~ 4900 ^{14}C yr, the turnover time
288 of DOC was much shorter. This is because ^{14}C age and turnover time ($1/k$, where $k = \Sigma(1/^{14}\text{C}$
289 age)) are equal only for a homogeneous C pool. For DOC composed of two pools with different
290 ^{14}C ages (e.g. 30 and 4900 ^{14}C yr), the turnover time ($284 \text{ yr} = 1/(0.1/30 + 0.9/4900)$) is much

291 less than its ^{14}C age due to dominance of the quickly cycled DOC term [*Loh et al.*, 2004;
292 *Trumbore and Druffel*, 1995].

293
294 The differences between the Atlantic DOC $\Delta^{14}\text{C}$ profiles presented here reveal that the DOC
295 cycle is far more dynamic, both spatially and temporally, than previously believed, particularly
296 in the North Atlantic. DOC $\Delta^{14}\text{C}$ values for samples collected from the SOce in 1995 [*Druffel*
297 *and Bauer*, 2000] have a lower average value ($-500 \pm 12\%$) below 1500m depth than those in
298 the North or South Atlantic, and are more variable. This suggests that more SOce measurements
299 are needed to constrain the cycling of DOC in the global ocean. We note that the biogeochemical
300 cycling of DOC is more clearly resolved when isotopic measurements are included vs.
301 concentration measurements alone. A more complete global picture of DOC cycling will be
302 further illuminated with future $\Delta^{14}\text{C}$ and compound specific $\Delta^{14}\text{C}$ measurements.

303

304

305 Acknowledgements

306 The authors gratefully acknowledge the technical assistance of Danielle Glynn and Christopher
307 Glynn, the advice and support of John Southon, the support of chief scientists Alison
308 MacDonald, Ruth Curry, and Molly Baringer, the guidance of Jim Swift, and the field support of
309 the crews of the R/V Atlantic and the NOAAAS Ronald H. Brown. We thank Francois Primeau for
310 his advice on deep ocean mixing. We thank Reiner Schlitzer for the 3D animation of DOC $\Delta^{14}\text{C}$
311 values (Alfred Wegener Institute, Helmholtz Centre for Polar and Marine Research,
312 Bremerhaven). This work was supported by the NSF Chemical Oceanography Program (OCE–
313 0961980 and OCE–141458941), the Kavli Foundation, the Keck Carbon Cycle AMS Laboratory,

314 and the NSF/NOAA-funded U.S. Repeat Hydrography Program. The data supporting the
315 conclusions can be obtained in the supporting information, and at the Repeat Hydrography Data
316 Center at the CCHDO website <http://cdiac.ornl.gov/oceans/RepeatSections/clivar.html>.

317

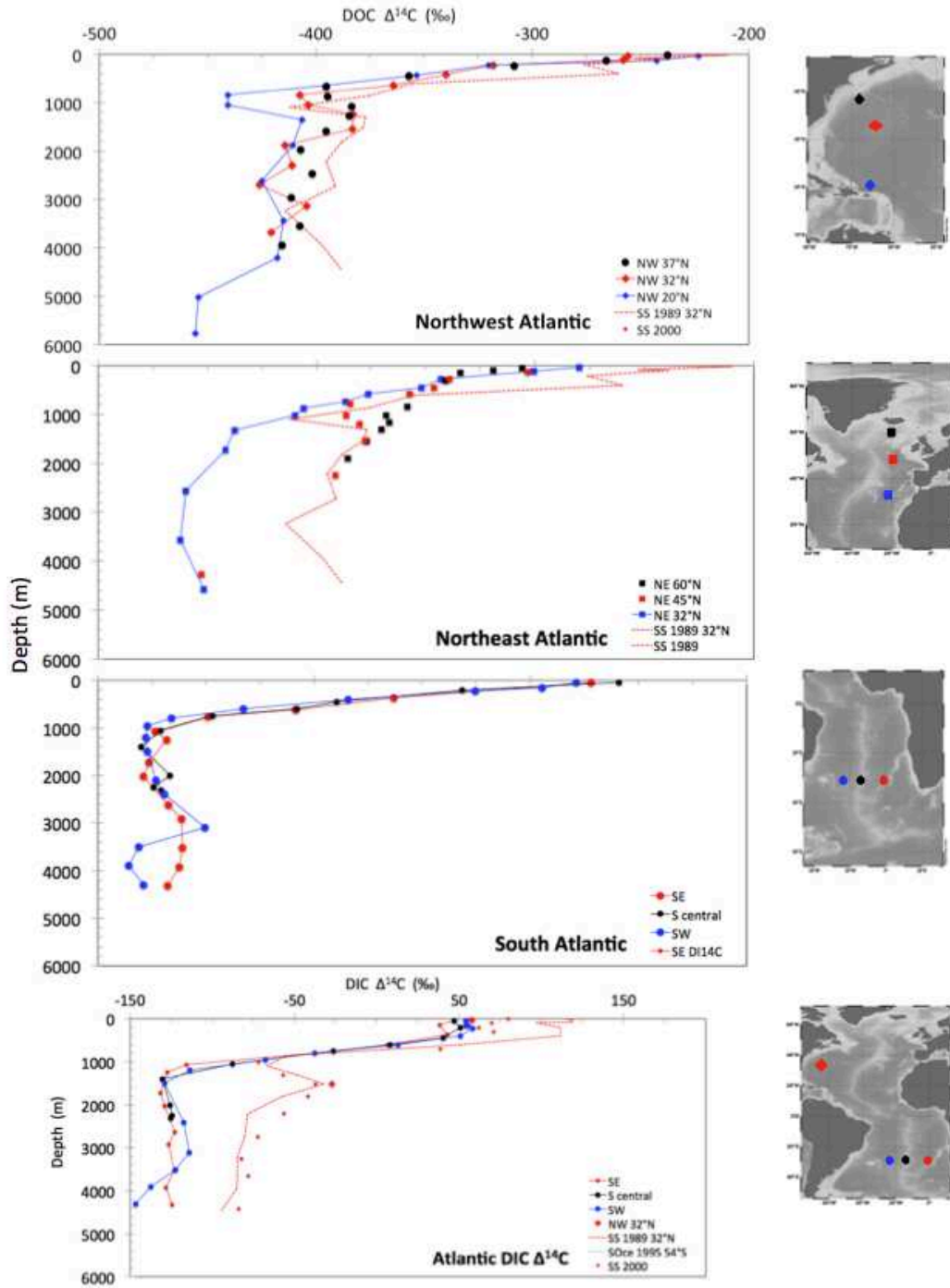
318 References

- 319 Bauer, J., and E. Druffel (1998), Ocean margins as a significant source of organic matter to
320 the deep open ocean, *Nature*, 392, 482-485.
- 321 Bauer, J., E. Druffel, P. Williams, D. Wolgast, and S. Griffin (1998), Inter- and intra-annual
322 variability in isotopic (^{14}C and ^{13}C) signatures of dissolved organic carbon in the eastern
323 North Pacific Ocean, *Journal of Geophysical Research*, 103, 2867-2882.
- 324 Beaupré, S., and E. Druffel (2009), Constraining the propagation of bomb-radiocarbon
325 through the dissolved organic carbon (DOC) pool in the northeast Pacific Ocean, *Deep-Sea
326 Research I*, 56, 1717-1726.
- 327 Beaupré, S., and L. Aluwihare (2010), Constraining the 2-component model of marine
328 dissolved organic radiocarbon, *Deep Sea Research II*, 57, 1493-1503.
- 329 Beaupré, S., E. Druffel, and S. Griffin (2007), A low-blank photochemical extraction system
330 for concentration and isotopic analyses of marine dissolved organic carbon, *Limnology and
331 Oceanography Methods*, 5, 174-184.
- 332 DeVries, T., and F. Primeau (2011), Dynamically and observationally constrained estimates
333 of water-mass distributions and ages in the global ocean, *Journal of Physical Oceanography*,
334 41, 2381-2401.
- 335 Druffel, E. (1989), Decade time scale variability of ventilation in the North Atlantic
336 determined from high precision measurements of bomb radiocarbon in banded corals,
337 *Journal of Geophysical Research*, 94, 3271-3285.
- 338 Druffel, E. (1996), Post-bomb radiocarbon records of surface corals from the tropical
339 Atlantic ocean, *Radiocarbon*, 38(3), 563-572.
- 340 Druffel, E., and J. Bauer (2000), Radiocarbon distributions in Southern Ocean dissolved and
341 particulate organic carbon, *Geophysical Research Letters*, 27, 1495-1498.
- 342 Druffel, E., and S. Griffin (2015), Radiocarbon in dissolved organic carbon of the South
343 Pacific Ocean, *Geophys. Res. Lett.*, 42, 4096-4101.
- 344 Druffel, E., P. Williams, J. Bauer, and J. Ertel (1992), Cycling of dissolved and particulate
345 organic matter in the open ocean, *Journal of Geophysical Research*, 97, 15639-15659.
- 346 Druffel, E., J. Bauer, S. Griffin, S. Beaupré, and J. Hwang (2008), Dissolved inorganic
347 radiocarbon in the North Pacific Ocean and Sargasso Sea, *Deep-Sea Research*, 55(4), 451-
348 459.
- 349 Druffel, E., S. Griffin, B. Walker, A. Coppola, and D. Glynn (2013), Total uncertainty of
350 radiocarbon measurements of marine dissolved organic carbon and methodological
351 recommendations, *Radiocarbon*, 55(2-3), 1135-1141.
- 352 Emerson, S. (2014), Annual net community production and the biological carbon flux in the
353 ocean, *Global Biogeochemical Cycles*, 28, 14-28.
- 354 Falkowski, P. (2014), The biogeochemistry of primary production in the sea, *Treatise on
355 Geochemistry (Second Edition)*, 10: Biogeochemistry, 163-187.
- 356 Fischer, J., M. Visbeck, R. Zantopp, and N. Nunes (2010), Interannual to decadal variability
357 of outflow from the Labrador Sea, *Geophys. Res. Lett.*, 37, doi:10.1029/2010GL045321.
- 358 Follett, C., D. Repeta, D. Rothman, L. Xu, and C. Santinelli (2014), Hidden cycle of dissolved
359 organic carbon in the deep ocean, *Proceedings of the National Academy of Sciences*, 111(47),
360 16706-16711.
- 361 Griffin, S., S. Beaupré, and E. Druffel (2010), An alternate method of diluting dissolved
362 organic carbon seawater samples for ^{14}C analysis, *Radiocarbon*, 52(2), 1224-1229.

363 Griffith, D., A. McNichol, L. Xu, F. McLaughlin, R. MacDonald, K. Brown, and T. Eglinton
364 (2012), Carbon dynamics in the western Arctic Ocean: insights from full-depth carbon
365 isotope profiles of DIC, DOC, and POC, *Biogeosciences*, 9, 1217-1224.
366 Hansell, D. (CA Carlson), 2001, *Deep-Sea Research II*, 48, 1649-1667.
367 Hansell, D., C. Carlson, and R. Schlitzer (2012), Net removal of major marine dissolved
368 organic carbon fractions in the subsurface ocean, *Global Biogeochemical cycles*, 26,
369 doi:10.1029/2011GB004069.
370 Jenkins, W. (2007), Tritium and helium-3 data from A22 cruise in 2003, edited by
371 CChdo.ucsd.edu/cruise, CCHDO.
372 Jenkins, W., S. S. Jr., E. Boyle, and G. Cutter (2015a), Water mass analysis for the U.S.
373 GEOTRACES (GA03) North Atlantic sections, *Deep Sea Research II*, 116, 6-20.
374 Jenkins, W., D. L. III, B. Longworth, J. Curtice, and K. Cahill (2015b), The distributions of
375 helium isotopes and tritium along the U.S. GEOTRACES North Atlantic sections
376 (GEOTRACESGA03), *Deep Sea Research II*, 116, 21-28.
377 Key, R., A. Kozyr, C. Sabine, K. Lee, R. Wanninkhof, J. Bullister, R. Feely, F. Millero, C. Mordy,
378 and T.-H. Peng (2004), A global ocean carbon climatology: Results from Global Data
379 Analysis Project (GLODAP), *Global Biogeochemical Cycles*, 18, doi:10.1029/2004GB002247.
380 Loh, A. N., J. E. Bauer, and E. R. M. Druffel (2004), Variable aging and storage of dissolved
381 organic components in the open ocean, *Nature*, 430, 877-881.
382 McNichol, A. P., G. Jones, D. Hutton, and A. Gagnon (1994), The rapid preparation of
383 seawater TCO₂ for radiocarbon analysis at the National Ocean Sciences AMS Facility,
384 *Radiocarbon*, 36(2), 237-246.
385 Mortazavi, B., and J. Chanton (2004), Use of Keeling plots to determine sources of dissolved
386 organic carbon in nearshore and open ocean systems, *Limnology and Oceanography*, 49(1),
387 102-108.
388 Reid, J. (1989), On the total geostrophic circulation of the South Atlantic Ocean: Flow
389 patterns, tracers and transports, *Progress in Oceanography*, 23, 149-244.
390 Schlitzer, R. (2015), 3D Scene of DOC $\Delta^{14}\text{C}$ in the World Ocean, edited, Alfred Wegener
391 Institute, Helmholtz Centre for Polar and Marine Research, **Bremerhaven**.
392 Smith, D., M. Simon, A. Alldredge, and F. Azam (1992a), Intense hydrolytic enzyme activity
393 on marine aggregates and implications for rapid particle dissolution, *Nature*, 359, 139-142.
394 Smith, D., M. Simon, A. Alldredge, F. A. I. hydrolytic, and e. a. o. m. a. a. i. f. r. p. dissolution
395 (1992b), Intense hydrolytic enzyme activity on marine aggregates and implications for
396 rapid particle dissolution, *Nature*, 359(6391), 139-142.
397 Southon, J. R., M. Santos, K. C. Druffel-Rodriguez, E. R. M. Druffel, S. E. Trumbore, S. G. X. Xu,
398 S. Ali, and M. Mazon (2004), The Keck Carbon Cycle AMS Laboratory, U.C.I.: Initial operation
399 and a background surprise, *Radiocarbon*, 46(1), 41-50.
400 Stuiver, M., and H. G. Ostlund (1980), GEOSECS Atlantic radiocarbon, *Radiocarbon*, 22, 1-24.
401 Stuiver, M., P. D. Quay, and H. G. Ostlund (1983), Abyssal water ^{14}C distribution and the age
402 of the world oceans, *Science*, 219, 849-851.
403 Tanaka, T., S. Ootosaka, M. Wakita, H. Amano, and O. Togawa (2010), Preliminary result of
404 dissolved organic radiocarbon in the western North Pacific Ocean, *Nuclear Instruments and*
405 *Methods in Physics Research B*, 268, 1219-1221.
406 Trumbore, S. E., and E. R. M. Druffel (1995), Carbon isotopes for characterizing sources and
407 turnover of non-living organic matter, in *Role of Nonliving Organic Matter in the Earth's*
408 *Carbon Cycle*, edited by R. Z. a. C. Sonntag, pp. 7-22, John Wiley & Sons, New York.

409 Williams, P. M., and E. R. M. Druffel (1987), Radiocarbon in dissolved organic carbon in the
410 central North Pacific Ocean, *Nature*, 330, 246-248.
411 Xu, X., S. Trumbore, S. Zheng, J. Southon, K. McDuffee, M. Luttgen, and J. Liu (2007),
412 Modifying a sealed tube zinc reduction method for preparation of AMS graphite targets:
413 Reducing background and attaining high precision, *Nuclear Instruments and Methods in*
414 *Physics Research B*, 259, 320-329.
415 Ziolkowski, L., and E. Druffel (2010), Aged black carbon identified in marine dissolved
416 organic carbon, *Geophysical Research Letters*, 37, 10.1029/2010GL043963.
417
418

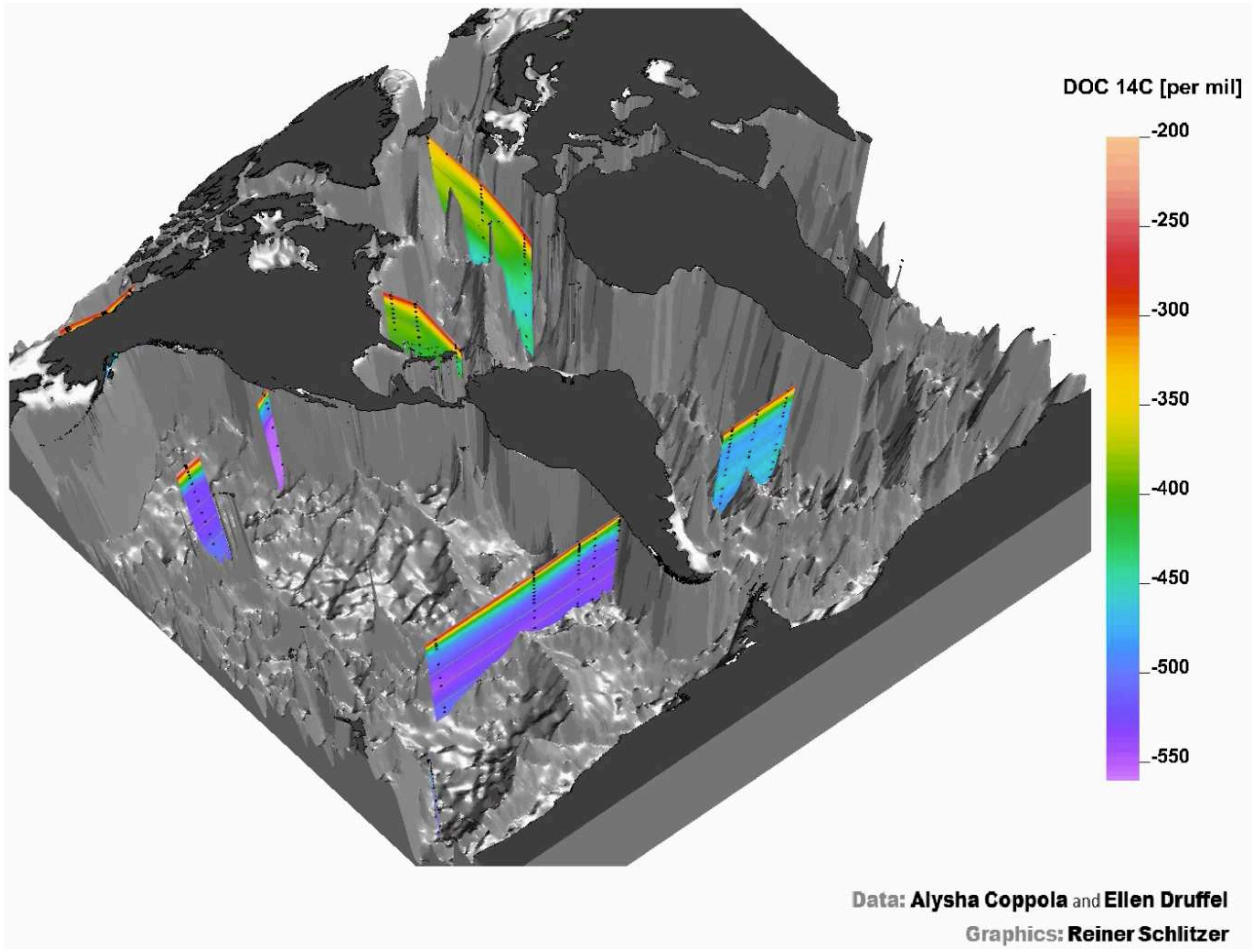
419 Figure 1. DOC $\Delta^{14}\text{C}$ values in samples collected from a) the northwest Atlantic along $\sim 65^\circ\text{N}$
 420 (A22 cruise 2012), b) the northeast Atlantic along $\sim 20^\circ\text{W}$ (A16N cruise 2013), and c) the South
 421 Atlantic along 32°S (A10 cruise 2011). d) DIC $\Delta^{14}\text{C}$ values in samples collected from the South
 422 Atlantic along 32°S (A10 cruise 2011) and the SS (A22 cruise in 2012 large red diamonds).
 423 DOC and DIC $\Delta^{14}\text{C}$ values from the SS (in 1989 [Druffel *et al.*, 1992] red dashed line are shown
 424 for comparison.
 425



426

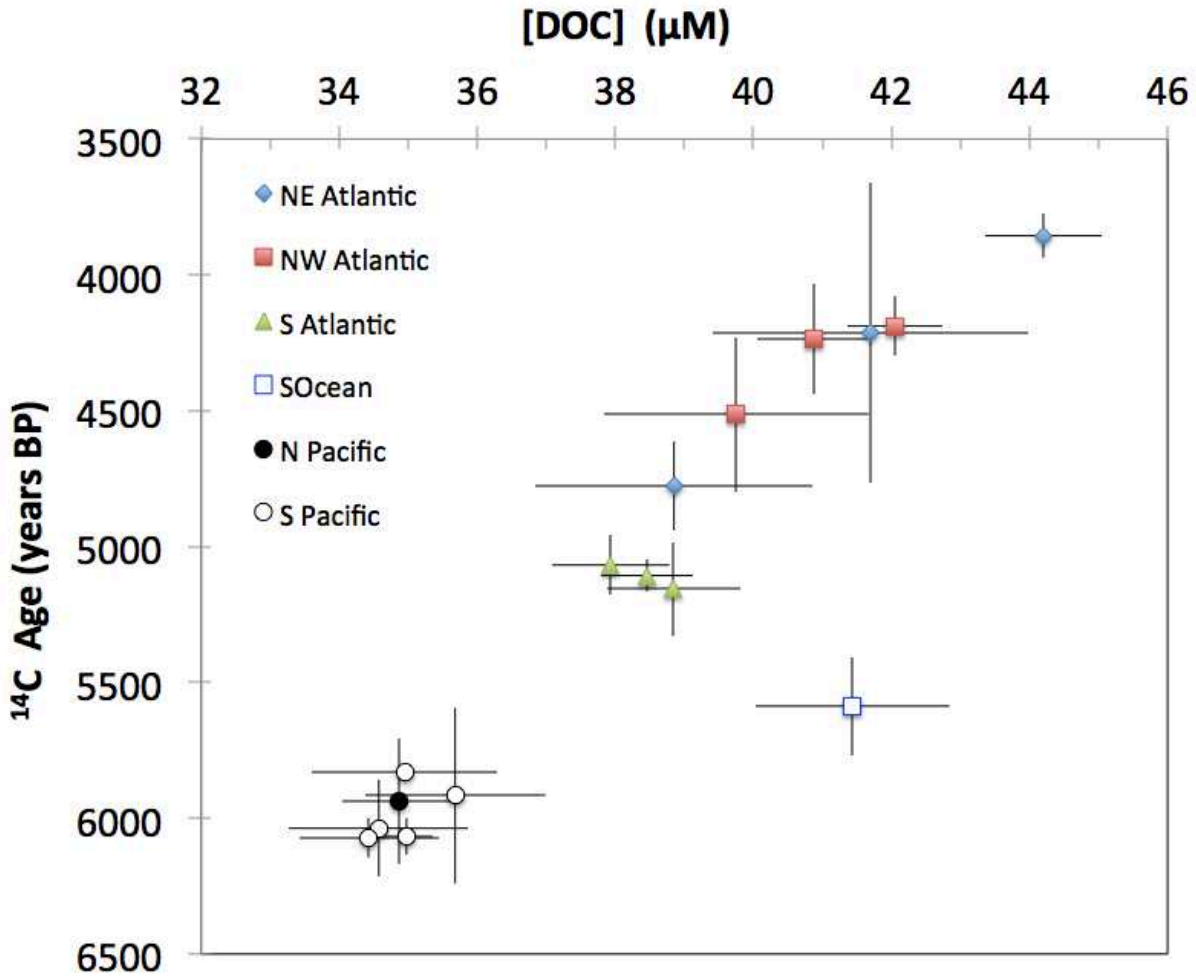
427
428
429
430
431

Figure 2. DOC 14C animation Three-dimensional animation produced by Reiner Schlitzer using Ocean Data View software.



432
433
434

435 Figure 3. DOC concentrations vs. DOC ^{14}C ages for samples >1500m depth. Data are from the
 436 Atlantic (this work), SS and north central Pacific [Druffel *et al.*, 1992], SOce ([Druffel and
 437 Bauer, 2000], and South Pacific [Druffel and Griffin, 2015]. Solid line is the Model II geometric
 438 mean regression of all points (except SOce), and dashed lines are the confidence limits (upper
 439 and lower 95%) that an individual point will fall on this line.
 440



441
 442